

# Model of Watershed Segmentation in Deep Learning Method to Improve Identification of Cervical Cancer at Overlay Cells

*by Sri Hadiani*

---

**Submission date:** 12-Sep-2023 09:48AM (UTC+0700)

**Submission ID:** 2163752958

**File name:** o\_Improve\_Identification\_of\_Cervical\_Cancer\_at\_Overlay\_Cells.pdf (1.01M)

**Word count:** 3660

**Character count:** 19575

# Model of Watershed Segmentation in Deep Learning Method to Improve Identification of Cervical Cancer at Overlay Cells

Dwiza Riana<sup>1,2</sup>, Muh Jamil<sup>1</sup>, Sri Hadiani<sup>1</sup>, Jufriadif Na'am<sup>1</sup>,  
Hadi Sutanto<sup>2,3</sup>, Ronald Sukwadi<sup>2,4</sup>

<sup>1</sup>Universitas Nusa Mandiri, Jalan Raya Jatiwaringin No 2, East Jakarta, Indonesia

<sup>2</sup>Universitas Katolik Indonesia Atma Jaya, Program Profesi Insinyur, Jalan Jendral Sudirman No.51, South Jakarta, Indonesia

<sup>3</sup>Atma Jaya Catholic University of Indonesia, Mechanical Engineering Masters Program, Jalan Jendral Sudirman No.51, South Jakarta, Indonesia

<sup>4</sup>Atma Jaya Catholic University of Indonesia, Industrial Engineering Study Program, Jalan Jendral Sudirman No.51, South Jakarta, Indonesia

**Abstract** – Cervical cancer is a disease that is very scary for women because it is the cause of death among women. To be aware of this disease is to do an early examination through the Pap Smear (PS) test. In terms of identifying overlapping cancer cells, still has low accuracy. Therefore, this research was carried out with the aim of getting the level of cell separation with high accuracy. This study uses a model to develop the Watershed segmentation technique in the Deep Learning Method. The data tested in this study comes from the RepomedUNM dataset. The amount of data tested is 420 overlapping images with the formulation of 1,260 test images. The results of this study can very well separate each overlapping cell with an average Intersection over Union (IoU) score of 0.9061. Each result can be divided fully by the whole of its area, so the final results of overlapping cells were successfully separated with an average score of 0.945. Therefore, this research can be used as a reference in identifying cervical cancer cells.

DOI: 10.18421/TEM122-26

<https://doi.org/10.18421/TEM122-26>

**Corresponding author:** Dwiza Riana,  
Universitas Nusa Mandiri, Jalan Raya Jatiwaringin No 2,  
East Jakarta, Indonesia  
**Email:** [dwiza@nusamandiri.ac.id](mailto:dwiza@nusamandiri.ac.id)

Received: 28 November 2022.

Revised: 16 March 2023.

Accepted: 10 April 2023.

Published: 29 May 2023.

© 2023 Dwiza Riana, Muh Jamil, Sri Hadiani, Jufriadif Na'am, Hadi Sutanto, Ronald Sukwadi; published by UIKTEN. This work is licensed under the Creative Commons Attribution-NonCommercial-NoDerivs 4.0 License.

The article is published with Open Access at <https://www.temjournal.com/>

**Keywords** – cervical cancer, Pap Smear, segmentation, deep learning, overlay cell.

## 1. Introduction

Cervical cancer (CC) is a disease that requires apprehension with it [1]. This cancer is one of the leading causes of death in women globally [2]. Most of the cells are relatively thin and lie beneath the surrounding tissue [3], making them very difficult to be identified [4].

The death rate due to CC can be significantly reduced by carrying out an early examination through the Pap Smear (PS) test [5]. The images from the results of these tests can be observed for abnormal cell conditions [6], but they tend to be very troublesome and are prone to errors when inspected manually [7]. For this reason, digital image processing techniques are needed to assist in sections so that high accuracy results are obtained.

There are still weaknesses in existing techniques, resulting in low accuracy for some cell classes [8]. The use of segmentation techniques for overlapping cells is still low [9]. Therefore, research in developing segmentation techniques to identify overlapping cells in CC images is needed. Cell segmentation on PS images is very important in identifying pre-cancerous changes in CC [10]. Several studies to segment CC cells have been carried out. The proposed method can work automatically or semi-automatically. Segmentation using the Mean-Shift clustering algorithm and Mathematical Morphology can identify cervical cell nuclei very effectively [11]. Selective-Edge-Enhancement-based Nuclei Segmentation method (SEENS) can achieve higher accuracy in cervical core segmentation [12].

The Circular Shape Function (CSF) technique works well in segmenting CC cell nuclei [13] and has a good accuracy using the Learning-based method [14]. Segmentation using the Watershed technique in identifying cell nuclei that overlaps with other cells does not have very good performance [15]. Therefore, this research was carried out with the support of the Deep Learning Method on Watershed.

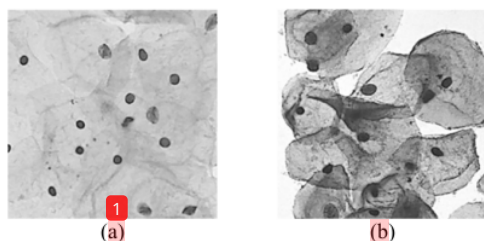


Figure 1. Dataset RepoMedUNM, (a). Normal, (b). Koilocyte

This method is used to detect and separate 2 cells that overlap with test data in the Repository medical image processing of Nusa Mandiri University (RepomedUNM). One of the test data is presented in Figure 1. The image presented in Figure 1 consists of 2 types, namely normal or uninfected cells and koilocyte or infected cells. Image is saved in Joint Photographic Expert (JPG) format, Grayscale type, with size of 512 x 512 pixels.

## 2. Research Methodology

In this research, integrated processes were carried out in one stage. The steps taken are presented in Figure 2.

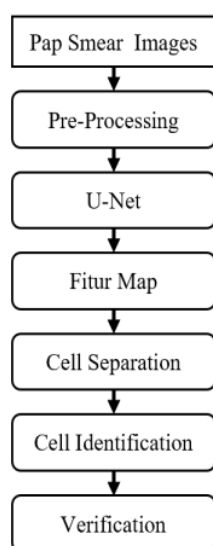


Figure 2. Stage of process

### A. Pap Smear Image

The images tested in this study were PS image datasets under normal and koilocyte conditions obtained from RepomedUNM. All images are in the form of digital images stored in the repository [17]. Many dataset images in this study are presented in Table 1.

Table 1. Number of Datasets

No	Type	Total
1	Normal	1,513
2	Koilocyte	420

### B. Pre-Processing

The pre-processing stage was carried out in two processes, namely augmentation and resizing. Augmentation aims to increase the shape of the image. The image will be rotated from the initial image form. The augmented image will be a new image, but does not change the meaning and value of the image itself. The process of augmentation is presented in Figure 3. The resulting image from the flip process was followed by a resize process, which was reducing it to the original image. This process aims to speed up the process and save resources. The resize formula is presented in Formula (1) and Formula (2).

$$nw = sr \left( \left( \frac{ow}{oh} \right) * ta \right) \quad (1)$$

$$nh = ta/nw \quad (2)$$

Where nw is the pixel width of the new image, ow is the pixel width of the original image, oh is the pixel height of the original image, ta is the desired area of the new image, and nh is the pixel height of the new image.

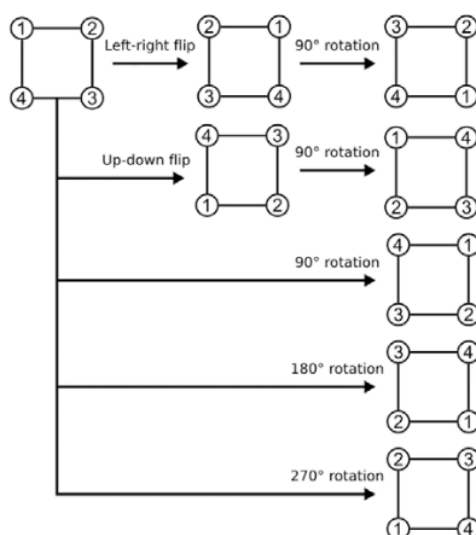


Figure 3. Process Augmentation [17]

### C. U-Net

U-Net is a semantic segmentation method that works by classifying pixels in an image [18]. U-Net requires 2 input images to produce an output image. The output image or raster image contains several bands and labels for each pixel [19]. The working concept of U-Net in this research is segmentation based on Deep Learning. The function of this method is to detect areas of cytoplasm and areas of overlapping cell [20], [21]. The U-Net method model used is presented in Figure 4.

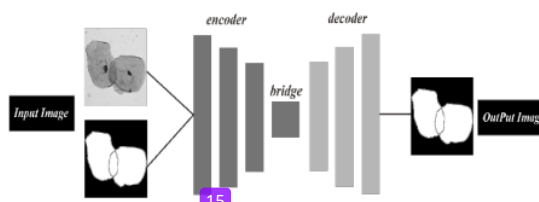


Figure 4. The U-Net Method Model

The U-Net model used in Figure 4 uses 3 types of encoders, namely Visual Geometry Group (VGG) [22], [23], Dense [24], and Mobile [25]. These three encoders become the VGG-UNet, Dense-UNet, and Mobile-UNet Architectures. Process results from all of these architectures will be verified in obtaining the level of accuracy.

### D. Map Feature

Feature map is the process of giving a consistent color in representing the cell area in the image [26]. The pixel values used consist of 3 colors, namely black with rgb values (0,0,0) for the background area, gray with rgb values (127,127,127) for cell edge areas, and white with rgb values (255,255,255) to represent cell area. Verification of the cell separation results uses a single cell label image with black rgb (0,0,0) to represent the background area and white rgb (255,255,255) to represent the cell area. An illustration of the results of the feature map process is presented in Figure 5.

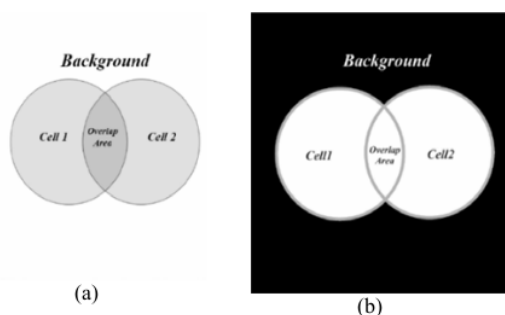


Figure 5. Map Feature Illustration, (a). Before, (b). After

### E. Cell Separation

Before the cell separation process was carried out, color distribution was implemented in each object area using the Watershed Segmentation Method. The border color in each object area will be represented as a catchment (basins). The midpoint in each area is represented as minima (lowest area).

After the foreground area has been successfully detected, each area will be connected and given an area marker with a different color. The resulting image is an image with area objects that have different colors, as illustrated in Figure 6.

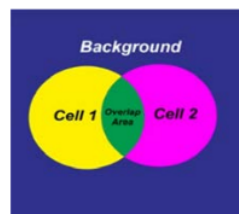


Figure 6. Color distribution using the Watershed Segmentation Method

Figure 6 is the result of giving different colors to each area that was successfully detected. There are only 4 colors that are owned by the image in all areas and the background area will be changed to black.

### F. Cell Identification

Cell identification is the process of taking cell area 1 and cell area 2 based on the color that has been given to the Cell Separation process. The color of Cell 1 is yellow, the color of Cell 2 will be changed to black, and the color of the overlapping area will be changed to yellow, as well as for the object of Cell 2. In this process, cell objects in the image can be identified correctly. An illustration of the results of this process is presented in Figure 7.

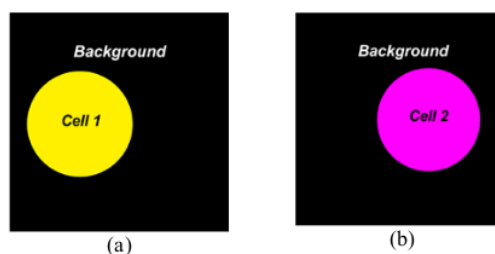


Figure 7. Illustration of Cell Separation, (a). Cell 1, (b). cell 2

### G. Verification

The verification is used in the form of generated performance metrics. Performance metrics are needed to see a picture between real conditions and the resulting predictions [27].



The performance matrix used to measure and verify the accuracy of the method consists of two, namely Intersection over Union (IoU) and Categorical Cross Entropy (CCE) Loss.

IoU is used to compare the similarity between 2 image properties. The properties that are compared are the width, height, and position into an area and volume of an object [28]. The IoU formula is presented in Equation (3).

$$IoU = \frac{|A \cap B|}{|A \cup B|} \quad (3)$$

CCE Loss is a metric used to calculate lost values. The CCE Loss formula is shown in Equation (4).

$$CCE\ Loss = \sum_{n=1}^n \left( a_i \log \log \frac{e^{Sp}}{\sum_i e^{Sp}} \right) \quad (4)$$

Where  $n$  is the number of classes,  $a_i$  is the actual probability, and  $Sp$  is the gradient for each predicted positive class.

### 3. Result and Discussion

This research was tested on 420 images containing 2 shapes of overlapping cell. Each image is augmented in the form of right and down flips, so the number of images tested is 1,260 images. This article presents one of the test images in grayscale format and a feature map. The image is presented in Figure 8.

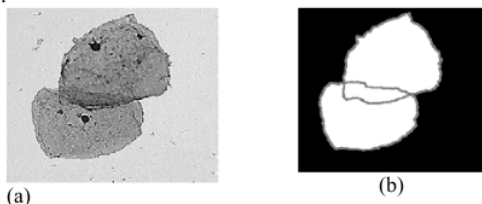


Figure 8. Koilocyte Image, (a). Grayscale, (b). Fitur Map

The image in Figure 8.a is an input image that has been converted into grayscale format. This image is engineered with a process of the feature map stage, so that the edge boundaries of each cell can be identified.

This image is augmented to rotate right and down. This process is used to increase the number of datasets in the segmentation process with deep learning to increase the value of segmentation accuracy. From the augmentation process, 420 x 3 images were obtained, namely 1,260 dataset images.

Image datasets in overlapping form are resized to 256 x 256 pixels which aims to reduce the computational burden in the training process. The U-Net model is used in this study can be seen in Figure 4.

This study used 50 epochs, hyperparameter optimizer adam, learning rate 0.0005, beta\_1 0.9,

beta\_2 0.999, epsilon 1e-07, and batch size 8 with a composition of 80% training data (1008 images) and 20% test data (252 images). The results of the IoU evaluation of the 3 U-Net architectures using Equation (3) are presented in Table 2.

Table 2. IoU verification results

Architecture	Background	Outline	Cell Area	Mean
VGG	0.9930	0.7554	0.9696	0.9061
Dense	0.9929	0.7440	0.9672	0.9014
Mobile	0.9919	0.7245	0.9636	0.8934

VGG-UNet and Dense-UNet verification scores do not have that much difference, but with Mobile-UNet, there is a significant difference. Verification with the Loss value using Equation (4) is presented in Table 3.

Table 3. Verification of CCE Loss

Architecture	Value
VGG-UNet	0.0381
Dense-UNet	0.0406
Mobile-UNet	0.0587

The loss score obtained from each architecture means that there are differences in the resulting image segmentation. A comparison of the resulting images is presented in Figure 9. Based on the scores obtained, the highest results were selected, namely the VGG-UNet segmentation of 252 as testing images that used the Watershed method.

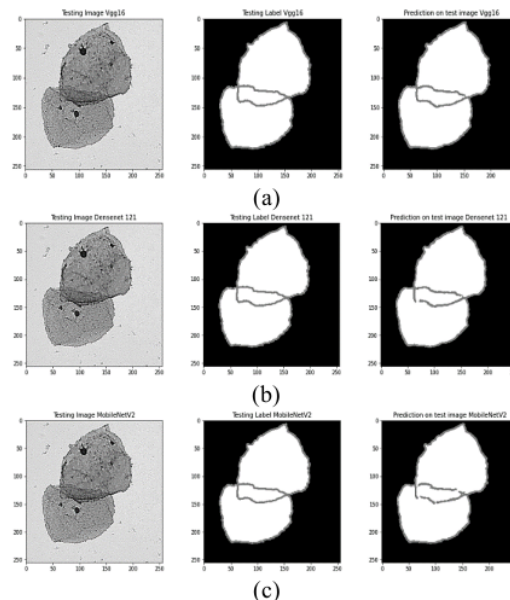


Figure 9. Comparison of segmentation results, (a). VGG-UNet, (b). Dense-UNet, (c). Mobile-UNet

Each area in the cell is given a different color so that it can be separated. The results of segmentation by giving color are presented in Figure 10.

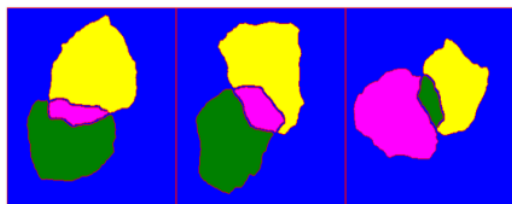


Figure 10. Segmentation results by coloring

Based on the color difference, each cell can be separated into a single cell. Each cell pixel value is selected and the verification  $V_{13}$  is calculated using IoU. The final segmentation results are presented in Table 4.

Table 4. Cell Separation Results

Label Image	Separation Results	IoU
		0.9749
		0.9695
		0.9705
		0.9677

The final results for the 252 separated testing images obtained an average IoU score of 0.945%. Next, the process of separating the overlay cells was carried out with the final results of segmentation for each cell presented in Table 5.

Based on the final results presented in Table 5, this method has shown significant results. Each overlaid cell can be separated according to clear size and shape which corresponds with a very high score.

Table 5. The final results of the overlay cell separation

Separation Results	Original image	Overlay Results

#### 4. Conclusion

This study has succeeded in proposing a new model for separating 2 overlapping cells in Pap smear images. The test results showed that VGG-UNet was able to outperform Dense-UNet and Mobile-UNet for multiclass segmentation images of cervical cells on Pap smear images. The average of IoU score is 0.9061 and the lowest loss is at 0.0381. The watershed method combined with the proposed U-Net method is proven to be able in separating each area in the image with a shape and accuracy very different term is needed. After separation, this model was able to obtain an average IoU score of 0.945%. Therefore, this research can be a reference in identifying cervical cancer cells correctly.

2

## Acknowledgments

The authors would like to thank the national competitive applied research grant of the Directorate General of Higher Education, Ministry of Education, Culture, Research, and Technology for supporting this research through "Repository Medical Imaging Pap Smear Images For Cervical Cancer Research In Indonesia Early Detection Of Cervical Cancer", 2022. The authors would like to thank the Lab Medik Khusus Patologi Anatomi Veteran Indonesia for the resource of RepoMedUNM database.

## References

- [1]. Hamama-Raz, Y., Shinan-Altman, S., & Levkovich, I. (2022). The intrapersonal and interpersonal processes of fear of recurrence among cervical cancer survivors: a qualitative study. *Supportive Care in Cancer*, 30(3), 2671-2678. Doi: 10.1007/s00520-021-06695-8
- [2]. Kassaman, D., Mushani, T., Kiraithe, P., Brownie, S., & Barton-Burke, M. (2022). Fear, faith and finances: health literacy experiences of English and Swahili speaking women newly diagnosed with breast and cervical cancer. *Ecancermedicalscience*, 16. Doi: 10.3332/ecancer.2022.1350
- [3]. Glasgow, H. L., Whitney, M. A., Gross, L. A., Friedman, B., Adams, S. R., Crisp, J. L., ... & Tsien, R. Y. (2016). Laminin targeting of a peripheral nerve-highlighting peptide enables degenerated nerve visualization. *Proceedings of the National Academy of Sciences*, 113(45), 12774-12779.
- [4]. Torres-Roman, J. S., Ronceros-Cardenas, L., Valcarcel, B., Bazalar-Palacios, J., Ybaseta-Medina, J., Carioli, G., ... & Alvarez, C. S. (2022). Cervical cancer mortality among young women in Latin America and the Caribbean: trend analysis from 1997 to 2030. *BMC public health*, 22(1), 1-10. Doi: 10.1186/s12889-021-12413-0
- [5]. Di Fiore, R., Suleiman, S., Drago-Ferrante, R., Subbannayya, Y., Pentimalli, F., Giordano, A., & Calleja-Agius, J. (2022). Cancer Stem Cells and Their Possible Implications in Cervical Cancer: A Short Review. *International Journal of Molecular Sciences*, 23(9), 5167. Doi: 10.3390/ijms23095167
- [6]. Riana, D., & Hidayanto, A. N. (2017). Integration of Bagging and greedy forward selection on image pap smear classification using Naïve Bayes. In *2017 5th International Conference on Cyber and IT Service Management (CITSM)* (1-7). IEEE. Doi: 10.1109/CITSM.2017.8089320
- [7]. Liu, W., Li, C., Xu, N., Jiang, T., Rahaman, M. M., Sun, H., ... & Grzegorzec, M. (2022). CVM-Cervix: A Hybrid Cervical Pap-Smear Image Classification Framework Using CNN, Visual Transformer and Multilayer Perceptron. *Pattern Recognition*, 130, 108829. Doi: 10.1016/j.patcog.2022.108829
- [8]. William, W., Ware, A., Basaza-Ejiri, A. H., & Obungoloch, J. (2018). A review of image analysis and machine learning techniques for automated cervical cancer screening from pap-smear images. *Computer methods and programs in biomedicine*, 164, 15-22. Doi: 10.1016/j.cmpb.2018.05.034
- [9]. Mustafa, W. A., Halim, A., Jamlos, M. A., & Idrus, S. Z. S. (2020). A Review: Pap smear analysis based on image processing approach. In *Journal of Physics: Conference Series*, 1529(2), 022080. IOP Publishing. Doi: 10.1088/1742-6596/1529/2/022080
- [10]. Song, Y., Cheng, J. Z., Ni, D., Chen, S., Lei, B., & Wang, T. (2016, April). Segmenting overlapping cervical cell in pap smear images. In *2016 IEEE 13th International Symposium on Biomedical Imaging (ISBI)* (1159-1162). IEEE. Doi: 10.1109/ISBI.2016.7493472
- [11]. Wang, P., Wang, L., Li, Y., Song, Q., Lv, S., & Hu, X. (2019). Automatic cell nuclei segmentation and classification of cervical Pap smear images. *Biomedical Signal Processing and Control*, 48, 93-103. Doi: 10.1016/j.bspc.2018.09.008
- [12]. Zhao, M., Wang, H., Han, Y., Wang, X., Dai, H. N., Sun, X., ... & Pedersen, M. (2021). Seens: Nuclei segmentation in pap smear images with selective edge enhancement. *Future Generation Computer Systems*, 114, 185-194. Doi: 10.1016/j.future.2020.07.045
- [13]. Saha, R., Bajger, M., & Lee, G. (2016, November). Spatial shape constrained fuzzy c-means (FCM) clustering for nucleus segmentation in pap smear images. In *2016 international conference on digital image computing: techniques and applications (DICTA)* (1-8). IEEE. doi: 10.1109/DICTA.2016.7797086
- [14]. Song, Y., Tan, E. L., Jiang, X., Cheng, J. Z., Ni, D., Chen, S., ... & Wang, T. (2016). Accurate cervical cell segmentation from overlapping clumps in pap smear images. *IEEE transactions on medical imaging*, 36(1), 288-300. Doi: 10.1109/TMI.2016.2606380
- [15]. Chankong, T., Theera-Umpon, N., & Auephanwiriyakul, S. (2014). Automatic cervical cell segmentation and classification in Pap smears. *Computer methods and programs in biomedicine*, 113(2), 539-556. Doi: 10.1016/j.cmpb.2013.12.012
- [16]. Mandiri, U., N. (2021). *Repository Medical Imaging Citra Pap Smear Untuk Deteksi Dini Cervical Cancer*, Universitas Nusa Mandiri. Retrieved from: <http://repomed.nusamandiri.ac.id/> [accessed: 05 March 2022]
- [17]. Sonogashira, M., Shonai, M., & Iiyama, M. (2020). High-resolution bathymetry by deep-learning-based image superresolution. *Plos one*, 15(7), e0235487. Doi: 10.1371/journal.pone.0235487
- [18]. Pun, N. S., & Agarwal, S. (2022). Modality specific U-Net variants for biomedical image segmentation: a survey. *Artificial Intelligence Review*, 55, 5845-5889. Doi: 10.1007/s10462-022-10152-1

- [19]. Jena, B., Nayak, G. K., Paul, S., & Saxena, S. (2022). An Exhaustive Analytical Study of U-Net Architecture on Two Diverse Biomedical Imaging Datasets of Electron Microscopy Drosophila ssTEM and Brain MRI BraTS-2021 for Segmentation. *SN Computer Science*, 3(5), 1-13. Doi: 10.1007/s42979-022-01347-y
- [20]. Riana, D., Hadianti, S., Rahayu, S., Hasan, M., Karimah, I. N., & Pratama, R. (2021, December). RepoMedUNM: A New Dataset for Feature Extraction and Training of Deep Learning Network for Classification of Pap Smear Images. In *International Conference on Neural Information Processing* (317-325). Springer, Cham. Doi: 10.1007/978-3-030-92307-5\_37
- [21]. Ronneberger, O. (2017). Invited talk: U-net convolutional networks for biomedical image segmentation. In Maier-Hein, geb. Fritzsche, K., Deserno, geb. Lehmann, T., Handels, H., Tolxdorff, T. (eds) *Bildverarbeitung für die Medizin 2017* (3-3). Springer Vieweg, Berlin, Heidelberg. Doi: 10.1007/978-3-662-54345-0\_3
- [22]. Mei, Y., Jin, H., Yu, B., Wu, E., & Yang, K. (2021). Visual geometry group-UNet: deep learning ultrasonic image reconstruction for curved parts. *The Journal of the Acoustical Society of America*, 149(5), 2997-3009. Doi: 10.1121/10.0004827
- [23]. Sathish, R., & Ezhumalai, P. (2021). Enhanced sentimental analysis using visual geometry group network-based deep learning approach. *Soft Computing*, 25(16), 11235-11243. Doi: 10.1007/s00500-021-05890-3
- [24]. Qamar, S., Ahmad, P., & Shen, L. (2021). Dense encoder-decoder-based architecture for skin lesion segmentation. *Cognitive Computation*, 13(2), 583-594. Doi: 10.1007/s12559-020-09805-6
- [25]. Jing, J., Wang, Z., Rättsch, M., & Zhang, H. (2022). Mobile-Unet: An efficient convolutional neural network for fabric defect detection. *Textile Research Journal*, 92(1-2), 30-42.
- [26]. Ponomarenko, N., Lukin, V., Egiazarian, K., Astola, J., Carli, M., & Battisti, F. (2008, October). Color image database for evaluation of image quality metrics. In *2008 IEEE 10th workshop on multimedia signal processing* (403-408). IEEE. Doi: 10.1109/MMSP.2008.4665112
- [27]. Rezatofighi, H., Tsoi, N., Gwak, J., Sadeghian, A., Reid, I., & Savarese, S. (2019). Generalized intersection over union: A metric and a loss for bounding box regression. In *Proceedings of the IEEE/CVF conference on computer vision and pattern recognition* (658-666). Doi: 10.1109/CVPR.2019.00075
- [28]. Yeung, M., Sala, E., Schönlieb, C. B., & Rundo, L. (2022). Unified Focal loss: Generalising Dice and cross entropy-based losses to handle class imbalanced medical image segmentation. *Computerized Medical Imaging and Graphics*, 95, 102026. Doi: 10.1016/j.compmedimag.2021.102026.



# Model of Watershed Segmentation in Deep Learning Method to Improve Identification of Cervical Cancer at Overlay Cells

## ORIGINALITY REPORT

12%

SIMILARITY INDEX

8%

INTERNET SOURCES

7%

PUBLICATIONS

1%

STUDENT PAPERS

## PRIMARY SOURCES

1

[jidt.org](http://jidt.org)

Internet Source

2%

2

[www.jatit.org](http://www.jatit.org)

Internet Source

2%

3

[www.mdpi.com](http://www.mdpi.com)

Internet Source

1%

4

Ruchika Arora, Indu Saini, Neetu Sood. "Multi-Label Segmentation and Detection of COVID-19 Abnormalities from Chest Radiographs Using Deep Learning", Optik, 2021

Publication

1%

5

[ijece.iaescore.com](http://ijece.iaescore.com)

Internet Source

1%

6

"Medical Image Computing and Computer Assisted Intervention – MICCAI 2019", Springer Science and Business Media LLC, 2019

Publication

1%

7	"Medical Image Understanding and Analysis", Springer Science and Business Media LLC, 2022 Publication	<1 %
8	Submitted to Vel Tech University Student Paper	<1 %
9	<a href="http://www.ncbi.nlm.nih.gov">www.ncbi.nlm.nih.gov</a> Internet Source	<1 %
10	<a href="http://coek.info">coek.info</a> Internet Source	<1 %
11	<a href="http://inass.org">inass.org</a> Internet Source	<1 %
12	<a href="http://unipress.bg">unipress.bg</a> Internet Source	<1 %
13	<a href="http://www.nature.com">www.nature.com</a> Internet Source	<1 %
14	S.M.A. Sharif, Rizwan Ali Naqvi, Farman Ali, Mithun Biswas. "DarkDeblur: Learning single- shot image deblurring in low-light condition", Expert Systems with Applications, 2023 Publication	<1 %
15	Sisi Wei, Hong Zhang, Chao Wang, Yuanyuan Wang, Lu Xu. "Multi-Temporal SAR Data Large-Scale Crop Mapping Based on U-Net Model", Remote Sensing, 2019 Publication	<1 %

16

Wasswa William, Andrew Ware, Annabella Habinka Basaza-Ejiri, Johnes Obungoloch. "A review of Image Analysis and Machine Learning Techniques for Automated Cervical Cancer Screening from pap-smear images", Computer Methods and Programs in Biomedicine, 2018

Publication

&lt;1 %

17

Zizhen Fan, Xiangchen Wu, Changzhong Li, Haoyuan Chen et al. "CAM-VT: A Weakly supervised cervical cancer nest image identification approach using conjugated attention mechanism and visual transformer", Computers in Biology and Medicine, 2023

Publication

&lt;1 %

18

ebin.pub

Internet Source

&lt;1 %

19

Yadavendra, Satish Chand. "Semantic segmentation of human cell nucleus using deep U-Net and other versions of U-Net models", Network: Computation in Neural Systems, 2022

Publication

&lt;1 %

Exclude quotes On

Exclude matches Off

Exclude bibliography On